Electronic Supplementary Information

CeO_2 Decorated Bimetallic Phosphide Nanowire Arrays for Enhanced Oxygen Evolution Reaction Electrocatalysis via Interface Engineering

Yikang Cong,[a] Xinnan Chen,[a] Yan Mei,[a] Jun Ye,[a] Ting-Ting Li[a,b,*]

[a]*School of Materials Science and Chemical Engineering, Ningbo 315211, China.*

[b]*Key Laboratory of Advanced Mass Spectrometry and Molecular Analysis of Zhejiang Province, Ningbo University, Ningbo 315211, China.*

[*]*Corresponding author：litingting@nbu.edu.cn (T.-T. Li)*

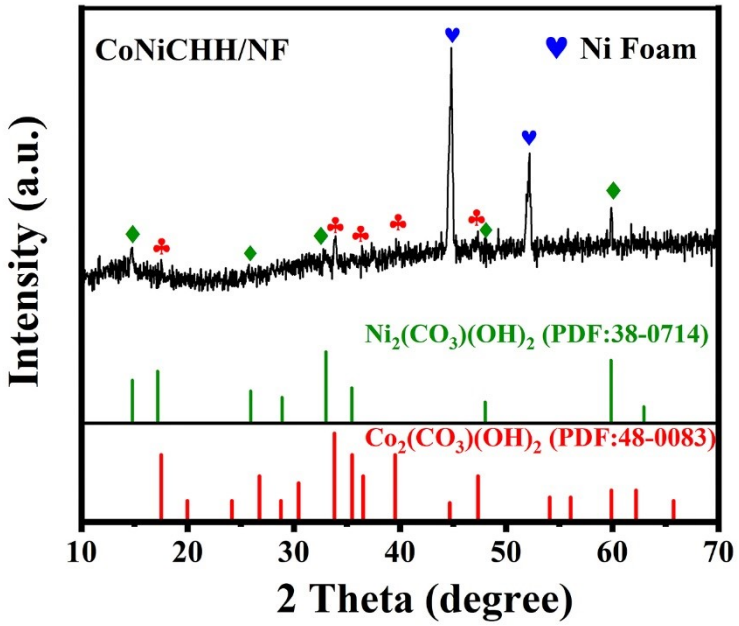

Fig. S1. XRD pattern of CoNiCHH/NF.

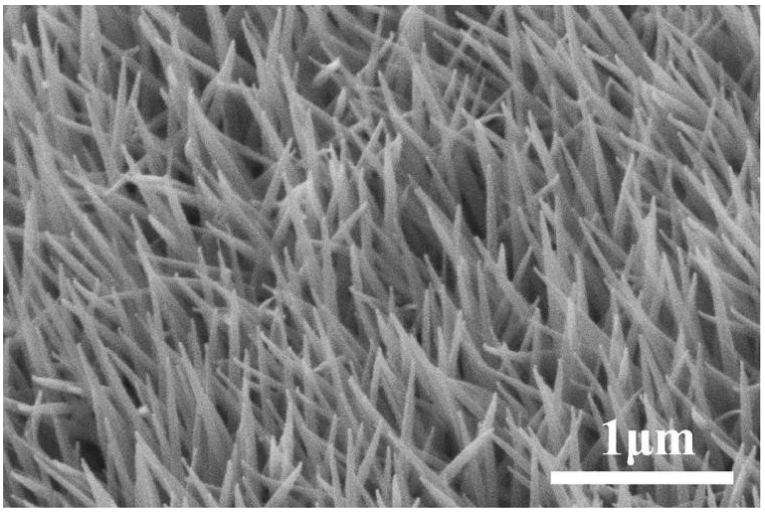

Fig. S2. SEM image of CoNiCHH/NF.

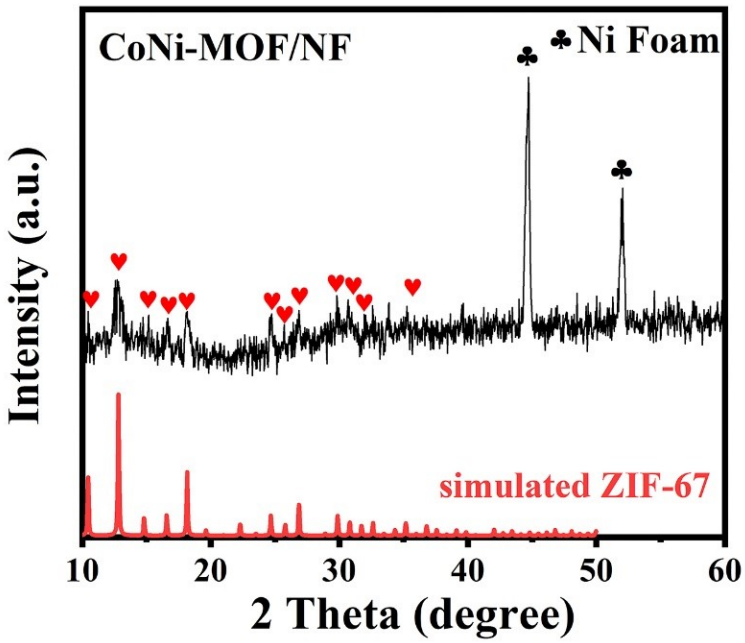

Fig. S3. XRD pattern of CoNi-MOF/NF

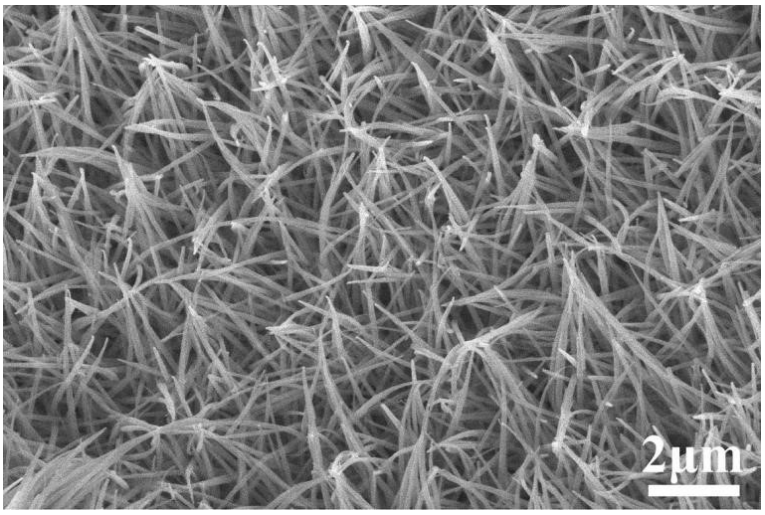

Fig. S4. SEM image of CoNi-MOF/NF.

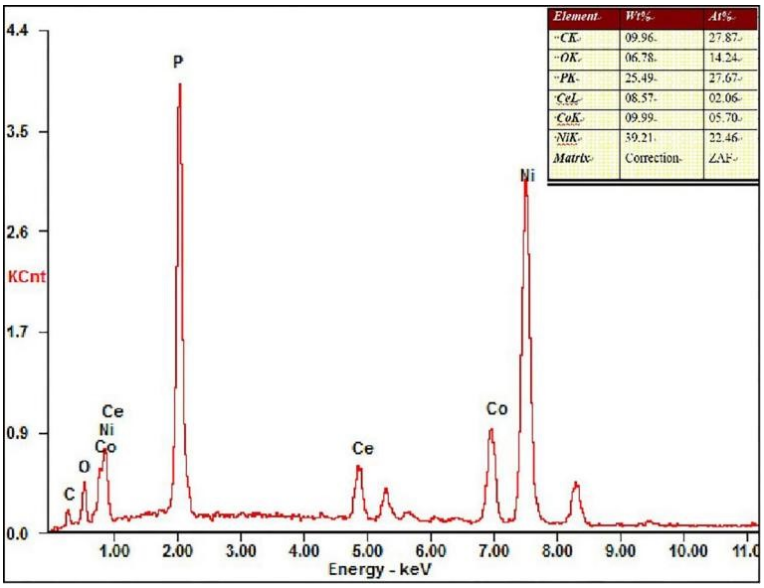

Fig. S5. EDX spectrum and elemental composition in $Co_{0.4}Ni_{1.6}P$-CeO_2/NF.

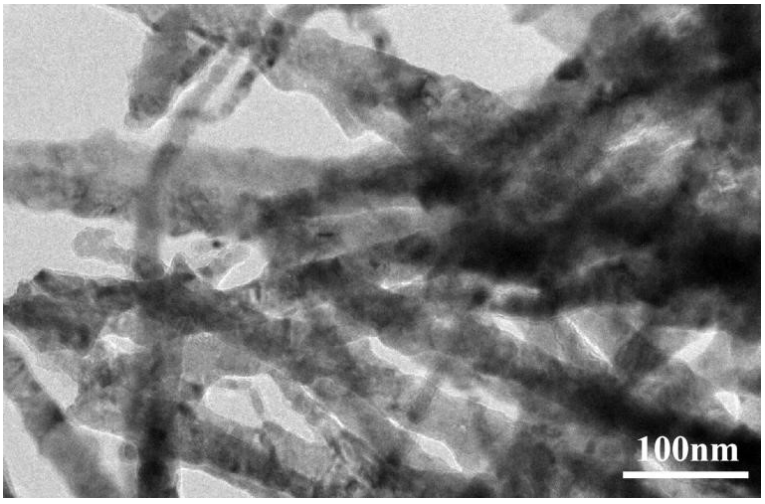

Fig. S6. TEM image of $Co_{0.4}Ni_{1.6}P$.

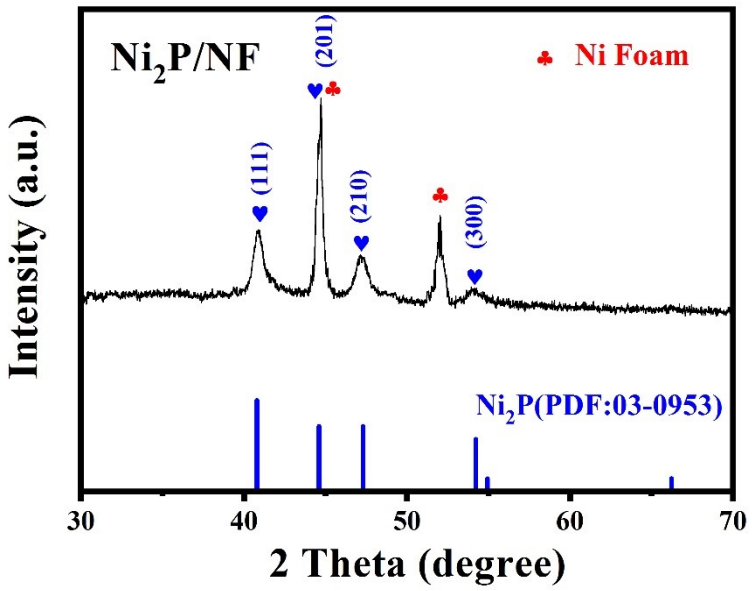

Fig. S7. XRD pattern of MOF-derived Ni_2P/NF.

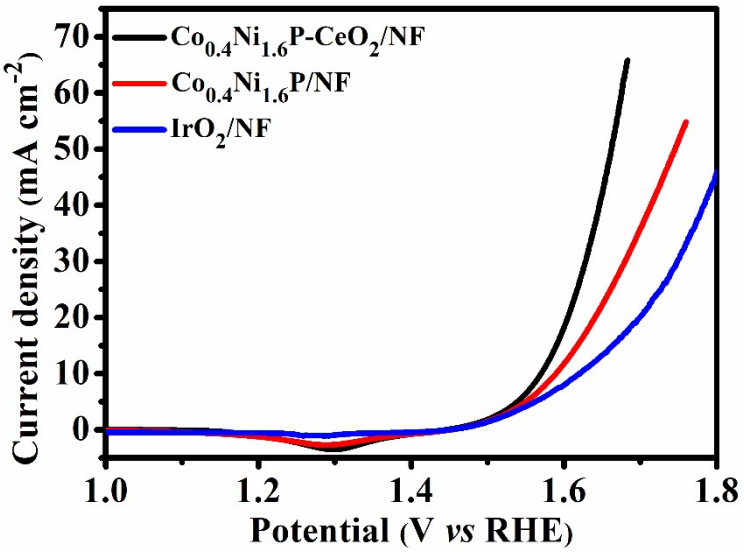

Fig. S8. The LSV plots of $Co_{0.4}Ni_{1.6}P$-CeO_2/NF, $Co_{0.4}Ni_{1.6}P$/NF, and IrO_2/NF in a neutral solution (0.1 M PBS, pH 6.8).

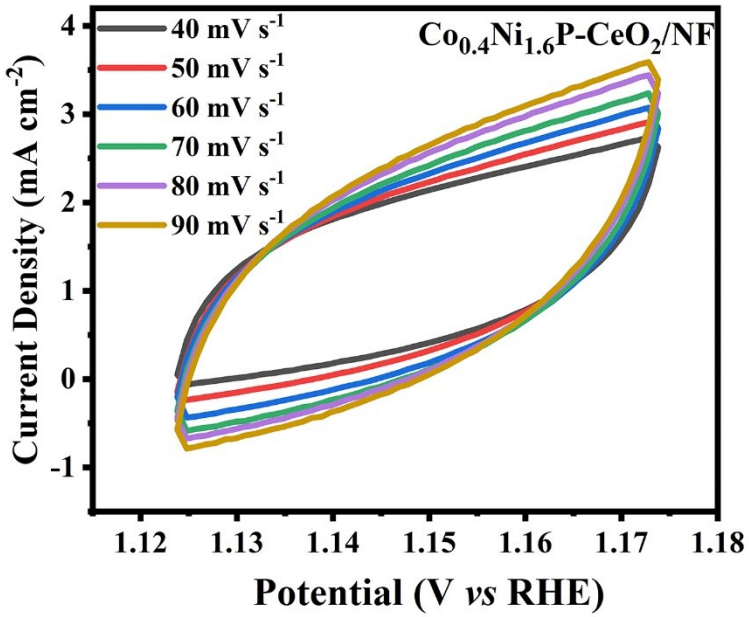

Fig. S9. Cyclic voltammograms of $Co_{0.4}Ni_{1.6}P$-CeO_2/NF measured at different scan rates.

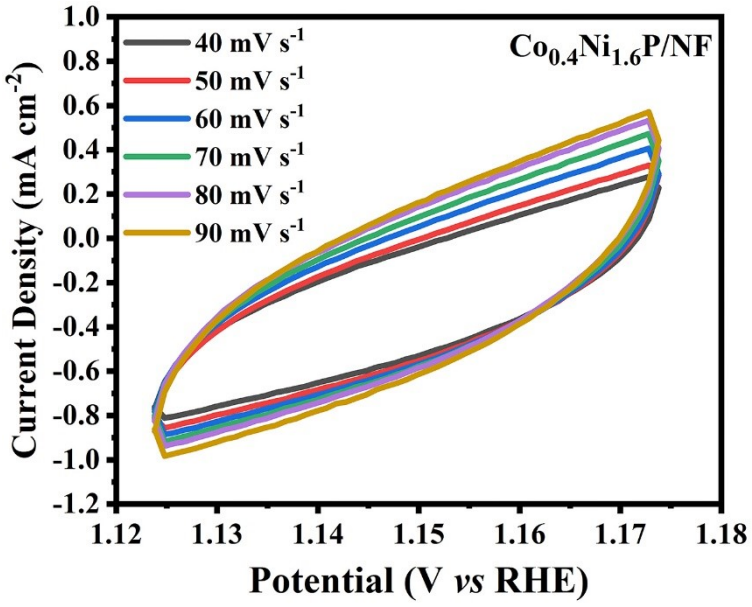

Fig. S10. Cyclic voltammograms of $Co_{0.4}Ni_{1.6}P$/NF measured at different scan rates.

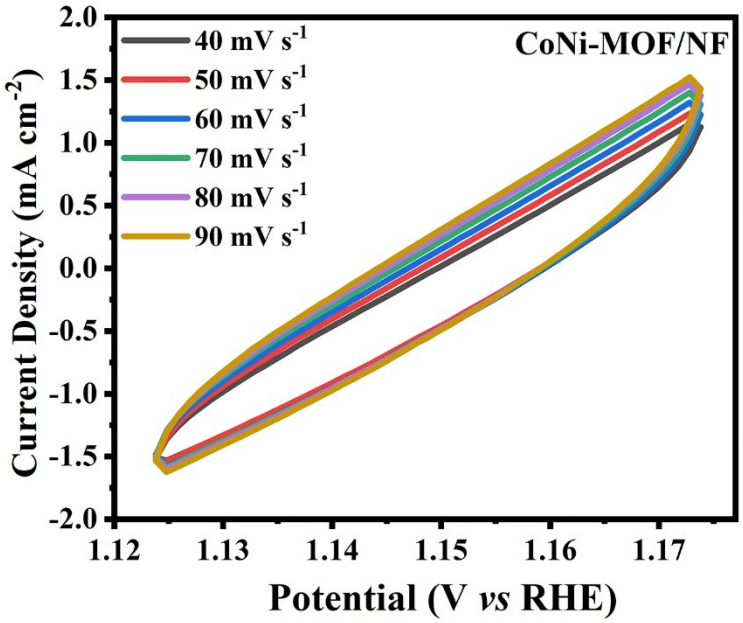

Fig. S11. Cyclic voltammograms of CoNi-MOF/NF measured at different scan rates.

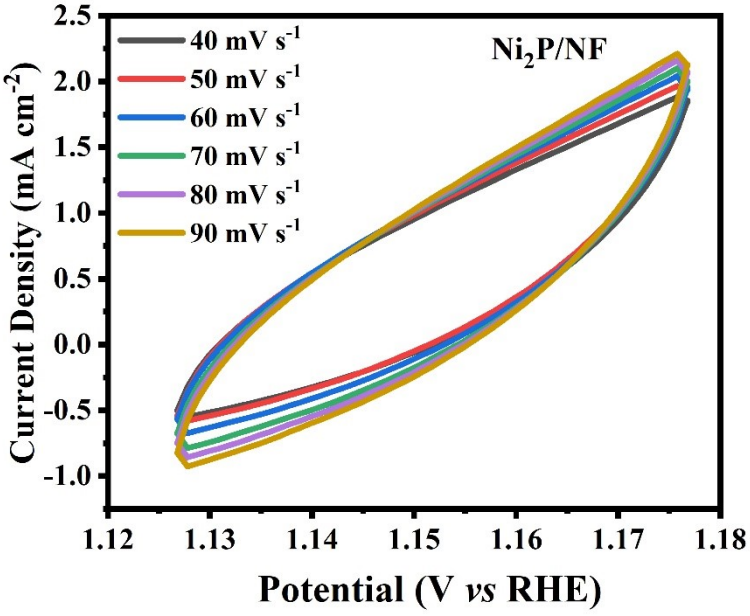

Fig. S12. Cyclic voltammograms of Ni_2P/NF measured at different scan rates.

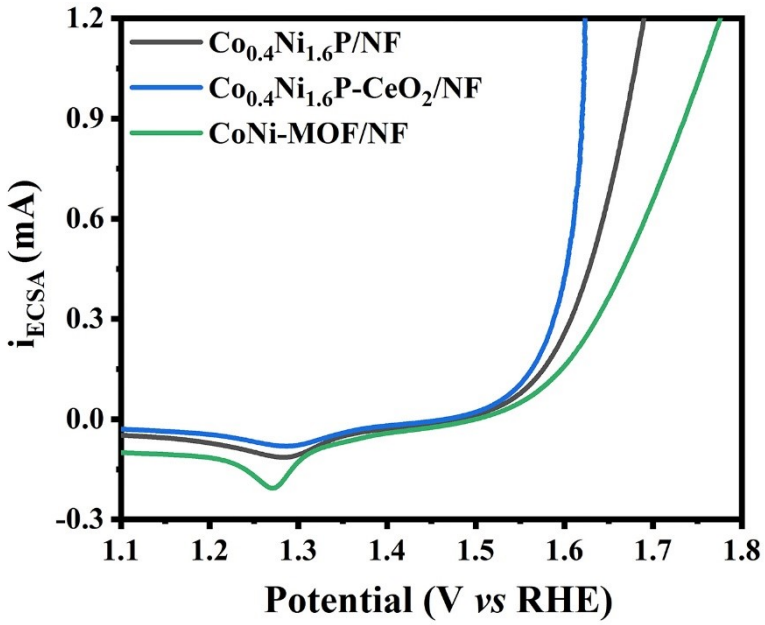

Fig. S13. OER polarization plots of $Co_{0.4}Ni_{1.6}P$-CeO_2/NF, $Co_{0.4}Ni_{1.6}P$/NF, and CoNi-MOF/NF normalized by the related ECSA values.

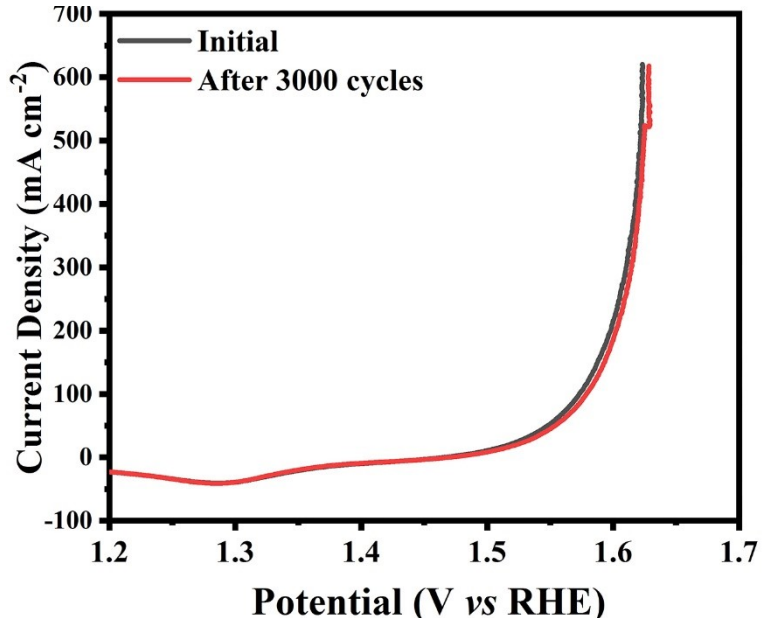

Fig. S14. The LSV curves recorded before and after 3000 cycles.

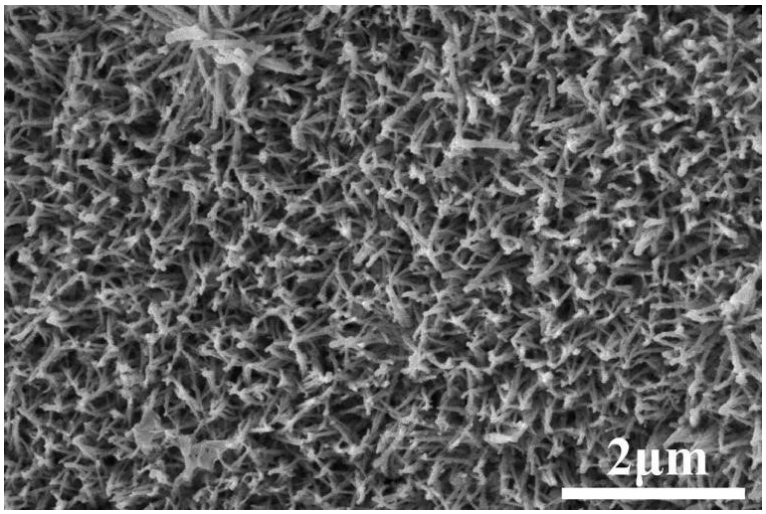

Fig. S15. SEM image of $Co_{0.4}Ni_{1.6}P$-CeO_2/NF after long-term stability test.

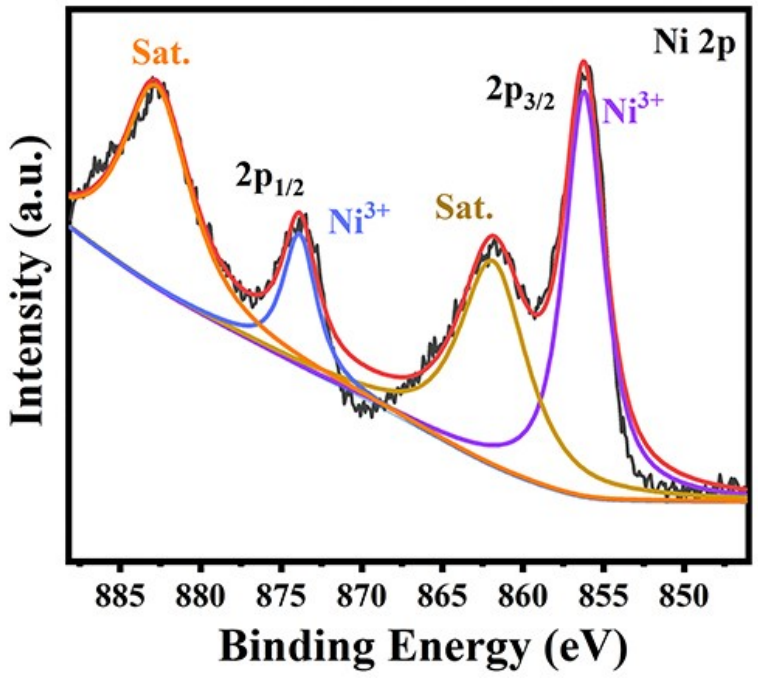

Fig. S16. Ni 2p XPS spectrum of $Co_{0.4}Ni_{1.6}P$-CeO_2/NF after 20 h stability test.

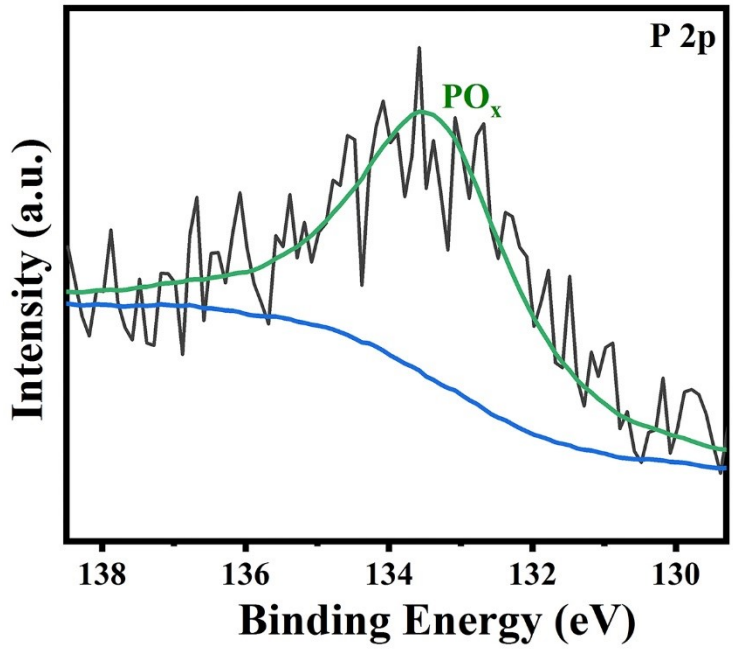

Fig. S17. P 2p XPS spectrum of $Co_{0.4}Ni_{1.6}P$-CeO_2/NF after 20 h stability test.

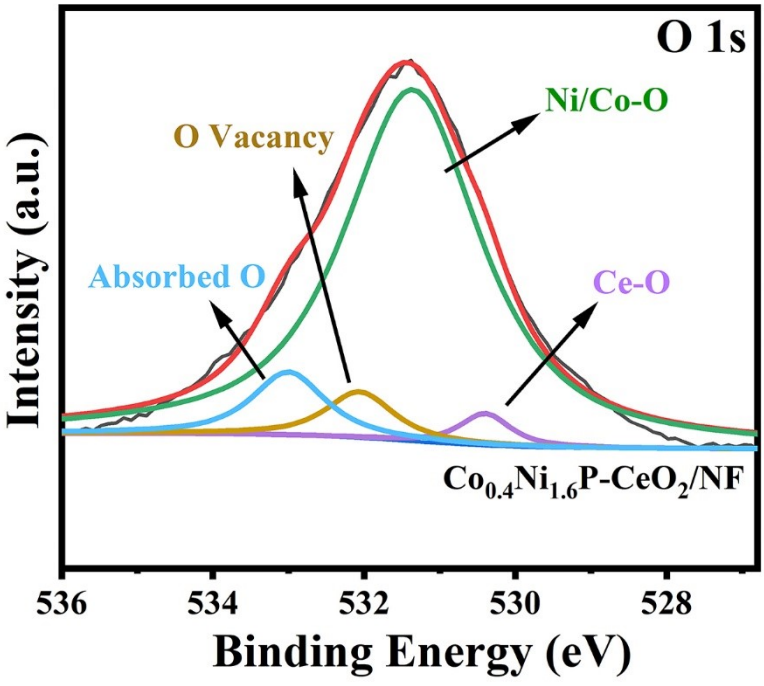

Fig. S18. O 1s XPS spectrum of $Co_{0.4}Ni_{1.6}P$-CeO_2/NF after 20 h stability test.

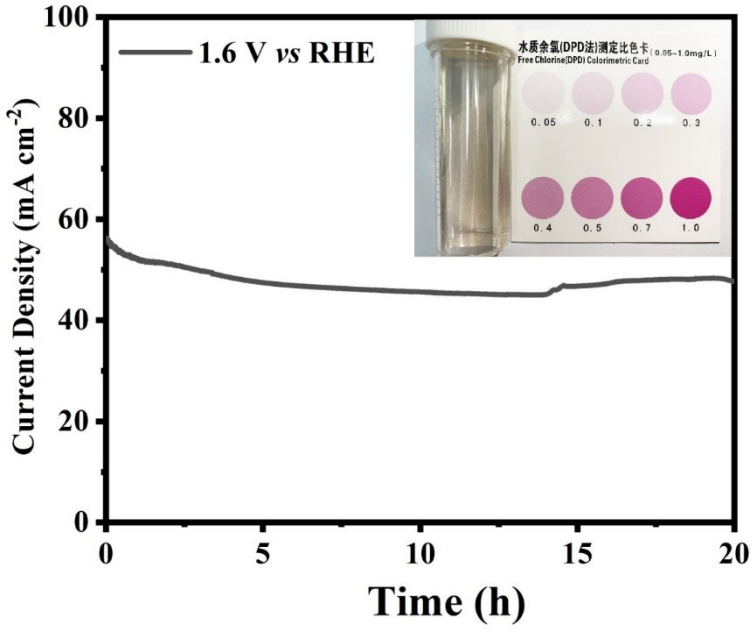

Fig. S19. Chronoamperometry curve of $Co_{0.4}Ni_{1.6}P$/NF at a fixed potential of 1.6 V *vs* RHE for 20 h.

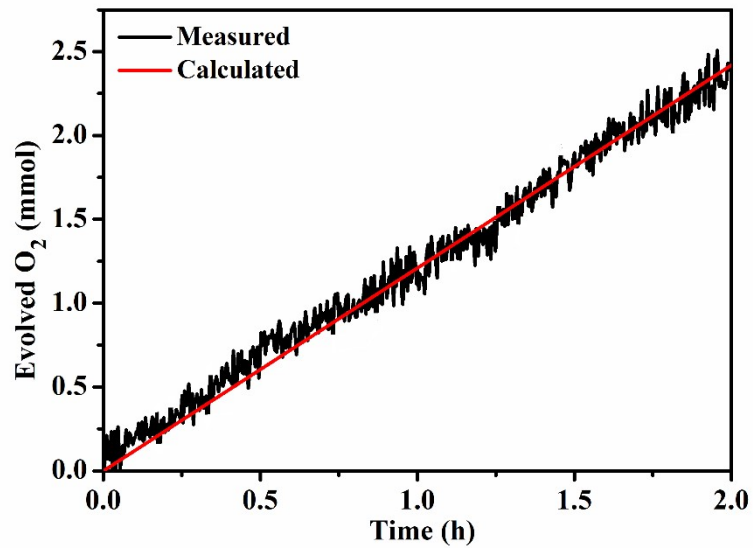

Fig. S20. The amounts of the theoretically calculated and experimentally measured O_2 *vs* electrolysis time for $Co_{0.4}Ni_{1.6}P$-CeO_2/NF at a constant potential of 1.6 V *vs* RHE during the initial 2 h.

Table S1. Comparisons of the electrocatalytic activities and stabilities of $Co_{0.4}Ni_{1.6}P$-CeO_2/NF and other CeO_2-based composites studied in previous studies.

Electrocatalysts	Electrolyte	η_{10} (mV)	η_{100} (mV)	Tafel slope (mV dec^{-1})	Ref.
$Co_{0.4}Ni_{1.6}P$-CeO_2/NF	1 M KOH	268	343	79.3	This work
CeO_2@Co_2N	1 M KOH	219	345	95.8	1
FeOOH/CeO_2	1 M KOH	230	—	92.3	2
CeO_x/$NiCo_2S_4$	1 M KOH	270	~530	126	3
CeO_x/CoS@L-CeO_2	1 M KOH	238	~370	42	4
CeO_2/$CoSe_2$	0.1 M KOH	288	—	44	5
CeO_x/CoO_x	1 M NaOH	313	—	66	6
CoP/CeO_2	1 M KOH	224	~380	90.3	7
h-Co_3O_4/CeO_2@N-CNFs	0.1 M KOH	310	—	89	8
Cu@CeO_2@NFC	1 M KOH	230.8	~340	32.7	9
CeO_2/Co_3O_4	1 M KOH	265	—	68.1	10
Ce-$MnCo_2O_4$	1 M KOH	337	—	125	11
CeO_x/CoS	1 M KOH	269	418	50	12
V-CoP@a-CeO	1 M KOH	230	480	48.1	13
Ce doping NiFe-LDH	1 M KOH	242	~380	34	14
CeO_2/$Co(OH)_2$	1 M KOH	410	~595	66	15
Ce-NiO-L	1 M KOH	382	~580	118.7	16
CeO_2@CeNC	1 M KOH	235	430	128.8	17
CeO_x/CoP/NF	1 M KOH	264	380	82	18

References

1 J. Zhang, W. He, H. B.Aiyappa, T. Quast, S. Dieckhöfer, D. Öhl, Y. T. Chen, J. Masa and W. Schuhmann, *Adv. Mater. Interfaces*, 2021, **8**, 2100041.

2 J. X. Feng, S. H. Ye, H. Xu, Y. X. Tong and G. R. Li, *Adv. Mater.,* 2016, **28**, 4698-4703.

3 X. Wu, Y. Yang, T. Zhang, B. Wang, H. Xu, X. Yan and Y. Tang, *ACS Appl. Mater. Interf.*, 2019, **11**, 39841-39847.

4 H. Xu, Y. Yang, X. Yang, J. Cao, W. Liu and Y. Tang, *J. Mater. Chem. A,* 2019, **7**, 8284-8291.

5 Y. R. Zheng, M. R. Gao, Q. Gao, H. H. Li, J. Xu, Z. Y. Wu and S. H. Yu, Small, 2015, **11**, 182-188.

6 J. H. Kim, K. Shin, K. Kawashima, D. H. Youn, J. Lin, T. E. Hong, Y. Liu, B. R. Wygant, J. Wang and G. Henkelman, *ACS Catal.*, 2018, **8**, 4257-4265.

7 M. Li, X. Pan, M. Jiang, Y. Zhang, Y. Tang and G. Fu, *Chem. Eng. J.*, 2020, **395**, 125160.

8 T. Li, S. Li, Q. Liu, Y. Tian, Y. Zhang, G. Fu and Y. Tang, *ACS Sust. Chem. Eng.*, 2019, **7**, 17950-17957.

9 J. Xia, H. Zhao, B. Huang, L. Xu, M. Luo, J. Wang, F. Luo, Y. Du and C. H. Yan, *Adv. Funct. Mater.*, 2020, **30**, 1908367.

10 B. Qiu, C. Wang, N. Zhang, L. Cai, Y. Xiong and Y. Chai, *ACS Catal.*, 2019, **9**, 6484-6490.

11 X. Huang, H. Zheng, G. Lu, P. Wang, L. Xing, J. Wang and G. Wang, *ACS Sustainable Chem. Eng.*, 2019, **7**, 1169-1177.

12 H. Xu, J. Cao, C. Shan, B. Wang, P. Xi, W. Liu and Y. Tang, *Angew. Chem., Int. Ed.,* 2018, **57**, 8654-8658.

13 L. Yang, R. Liu and L. Jiao, *Adv. Funct. Mater.,* 2020, **30**, 1909618.

14 H. Xu, C. Shan, X. Wu, M. Sun, B. Huang, Y. Tang and C. H. Yan, *Energy Environ. Sci.,* 2020, **13**, 2949-2956.

15 M. C. Sung, G. H. Lee and D. W. Kim, *J. Alloys Compd.*, 2019, **800**, 450-455.

16 W. Gao, Z. Xia, F. Cao, J. C. Ho, Z. Jiang and Y. Qu, *Adv. Funct. Mater.*, 2018, **8**, 1706056.

17 B. Wang, P. Xi, C. Shan, H. Chen, H. Xu, K. Iqbal, W. Liu and Y. Tang, *Adv. Mater. Interfaces*, 2017, **4**, 1700272.

18 T. Zhang, X. Wu, Y. Fan, C. Shan, B. Wang, H. Xu and Y. Tang, *ChemNanoMat*, 2020, **6**, 1119-1126.